

Article

Manufacturing and Assessment of Electrospun PVP/TEOS Microfibres for Adsorptive Heat Transformers

Patrizia Frontera ¹, Mikio Kumita ², Angela Malara ¹, Junya Nishizawa ²
and Lucio Bonaccorsi ^{1,3,*}

¹ Department of Civil, Energetic, Environmental and Materials Engineering, Mediterranean University of Reggio Calabria, 89134 Reggio Calabria, Italy

² Graduate School of Natural Science and Technology, Kanazawa University, Kakuma-machi, 920-1192 Kanazawa, Japan

³ CNR-ICCOM, Via G. Moruzzi 1, 56124 Pisa, Italy

* Correspondence: lucio.bonaccorsi@unirc.it; Tel.: +39-965-169-2309

Received: 7 June 2019; Accepted: 11 July 2019; Published: 16 July 2019



Abstract: A new adsorbent coating for the adsorber unit of an adsorption heat pump made of hybrid, organic–inorganic microfibres was prepared and characterized. Different coatings were obtained by the electrospinning of polyvinylpyrrolidone (PVP) solutions added with different quantities of tetraethyl orthosilicate (TEOS). PVP is a polymer with water adsorption capability and the TEOS addition allowed to increase the thermal stability of microfibres. The aim, indeed, was to preserve the polymeric structure of microfibres in order to obtain coatings with high flexibility and mechanical strength. The results demonstrated that TEOS concentrations in the range of 5–13 wt.% produced microfibre coatings of non-woven textile structure with both good water affinity and good thermal stability. SEM images of coatings showed that the deposited microfibre layers have both a high surface area and a high permeability representing a significant advantage in adsorption systems.

Keywords: electrospinning; adsorption; microfibre coatings; polyvinylpyrrolidone

1. Introduction

Electrospinning is a technique to produce fibres of sub-micrometric diameter by a relatively simple and inexpensive method [1–3]. During the process, a jet of microfibres is continuously ejected towards a collector, thus forming a non-woven mat covering the surface [4,5]. The material typically used in electrospinning is a polymeric solution and there are many applications in which electrospun microfibres can be used, as demonstrated by the numerous patents and publications even in the medical and biomedical fields [6–8]. Large surface area, mechanical strength, surface functionality, flexibility, and shape adaptability are some of the characteristics that make microfibre textiles interesting materials for new and traditional applications. In this work, electrospinning has been used to prepare an innovative functional coating made of hybrid microfibres for adsorption heat pump systems. Adsorption heat transformers are eco-friendly and sustainable systems for refrigeration and cooling. Their functioning is based on the cyclic adsorption/desorption of water vapor on a porous solid that acts, in collaboration with an evaporator and a condenser, as the compressor in a traditional heat pump replacing mechanical energy with thermal energy [9,10]. In order to drive the inverse thermodynamic cycle of an adsorption pump, an additional heat source is needed, generally based on waste heat recovery [11]. Detailed descriptions of adsorption heat pumps and their thermodynamic operation are reported in the literature [9,12,13]. The traditional porous materials used in solid sorption applications are zeolites and silica gel. Zeolites are characterized by a network of linked alumina

and silica tetrahedra that form a crystalline nanoporous structure with hydrophilic behavior [14,15]. Although zeolites are the ideal adsorbing solid for the elevated thermal stability, their use in adsorption systems is limited by the high regeneration temperatures. The desorption of water vapor from the zeolite porosity requires temperatures above 300 °C for the complete material dehydration [16,17]. The ideal exploitation of this technology, indeed, is the coupling with low temperature heat sources ($T < 150$ °C), like solar thermal panels or waste combustion fumes [11,18]. For such a reason, other adsorbing materials have been proposed and sometimes used in solid sorption applications, like silica gel, aluminophosphates (AIPO and SAPO), and metalorganic frameworks (MOF). AIPO and SAPO are interesting for their high adsorption capacity, their good structural stability, and low regeneration temperatures but they are difficult to find on the market and costly [19,20]. MOF are new adsorbing materials with large water capacity and low regeneration temperatures, but their structural stability is still an open issue and they are expensive and difficult to find in large quantities [21,22]. Among others, silica gel is the adsorbent most used in commercial adsorption chillers mainly for its low cost and large availability on the market although it shows a lower water adsorption capacity and problems of morphological and thermal stability [22–25].

Over the years, the scientific community has focused not only on the development of the porous material but also on the engineering of the absorber, the heat exchanger module where the adsorbent material is located. In order to reduce heat transfer resistances, the porous material distribution around the heat exchanger surfaces is very important. Zeolites and silica gel are generally used in form of granules or powder and the simplest and most used solution is to fill the free space between the fins of the heat exchanger with the adsorbent granules. In this case, however, the poor contact between the adsorbent particles and the metallic surfaces causes high thermal resistances at the interface [26]. More recent developments have shown that better performances are obtained when the adsorbing solid is shaped as a coating covering the heat exchanger surfaces. A coating has several advantages compared to the loose powder because the interface contact is improved and the quantity of porous material needed is optimized as well as the mechanical and thermal stability of the adsorber module [27,28]. Several different solutions have been proposed, like the direct synthesis of the adsorbing material on the heat exchanger surfaces [29,30] or the use of binders and ligands to make coatings [23,31] or the use of metallic or polymeric fibres or foams [32–35]. Each of these solutions, however, has many restrictions due to the scale up to an industrial level maintaining competitive production costs. For these reasons the commercial heat pumps and chillers are still made with granules and pellets.

The novelty of the coating presented in this work consists of three principal features: the material, which is based on polyvinylpyrrolidone (PVP) modified with tetraethyl orthosilicate (TEOS), the coating structure, which is made of layers of non-woven microfibres and the coating technique used, based on the electrospinning. PVP is a material known for its good biocompatibility and non-toxicity [36,37], largely used as additive in medical, food, and cosmetic products due to its optimal interaction with water and a wide range of organic and inorganic compounds [38,39]. PVP is easily spinnable and has been frequently used to produce electrospun microfibres for scaffolds, membranes, and filtering materials [2,6,40]. PVP and other polymers have been already used to prepare silica nanofibers with the role of carriers for silanol groups. The polymeric carrier is successively decomposed by calcination in order to leave the inorganic fibrous structure [41,42]. The pure silica microfibres obtained in this way, however, would be too brittle to be used as coatings for adsorption heat transformers in which mechanical stability is an important issue. In the fibrous coating presented in this work, the hybrid, organic–inorganic nature of microfibres has been preserved by maintaining the PVP polymeric structure and bonding tetraethyl orthosilicate (TEOS) to ensure thermal stability, structural flexibility, and long-term usability without compromising the adsorbent properties.

2. Materials and Methods

2.1. Electrospinning of Hybrid Microfibres

Microfibres have been prepared by electrospinning of mixtures of polyvinylpyrrolidone (PVP, Molecular weight 1300000, Sigma Aldrich, Saint Louis, MO, USA) and tetraethyl orthosilicate (TEOS 99.9%, Sigma Aldrich). A typical solution for electrospinning was prepared dissolving 1 g of PVP powder in 5 g of ethanol at room temperature and stirred at 500 rpm for 30 min. TEOS was then added to the solution (at room temperature) and the mixture was left stirring overnight. The amounts of silicate added are shown in Table 1.

Table 1. Precursor solutions for electrospinning.

Sample	TEOS in the PVP/EtOH Sol. (wt.%)
Mf-0	0
Mf-5	5
Mf-8	8
Mf-13	13
Mf-18	18
Mf-24	24

The PVP/TEOS/EtOH precursor mixture was loaded in a 10 mL syringe fitted with a 1 mm steel needle and electrospun at a flow rate of 1.2 mL/h with an applied voltage of 13.5 kV (kdScientific Model 100, Electro-spinner 2.0, Linari Engineering s.r.l., Pisa, Italy). The collector distance was fixed at 15 cm from the needle.

2.2. Microfibres Characterization

The silica microfibres were morphologically characterized by scanning electron microscopy, SEM (Phenom ProX, Thermo Fisher Scientific, Waltham, MA, USA), and the chemical composition measured by the microscope EDX microprobe. Morphological characteristics of microfibres were evaluated by digital image analysis by the software ImageJ (v 1.52a) and the plugin DiameterJ (v 1.018) [43], specifically developed for nanofibres characterization. Thermal stability of samples was analyzed by thermogravimetry-differential scanning calorimetry, TGA-DSC, (STA 409 PC Netzsch, Selb, Germany) from 25 to 700 °C in airflow with a heating rate of 10 °C/min.

3. Results and Discussion

PVP is a polymer showing good water affinity. In adsorption systems, however, the structural stability of the adsorbing material is a key issue: under cyclic water adsorption/desorption the material should not show structural modifications that could compromise the operational functioning of the adsorption machine. The objective of the TEOS addition to PVP was to improve the thermal stability of the polymeric chains. For such a reason, microfibres with different contents of TEOS have been prepared and assessed as discussed below.

3.1. Microfibres Morphological Characterization

The result of the electrospinning action on a collector surface is the formation of a continuous coating of microfibres which form a non-woven fabric of the desired thickness. SEM images of microfibre samples at different silicate concentrations, from Mf-0 to Mf-24, are shown in Figure 1. Sample Mf-0 is made of pure PVP microfibres without TEOS addition obtained by the electrospinning of a PVP solution of 16.7 wt.% in ethanol. This PVP concentration was selected from a set of experiments carried out to find the ideal electrospinning conditions. The pure PVP coating (Mf-0 in Figure 1) shows regular-shaped microfibres with lengths of a few millimeters and micrometric diameters. The average diameters obtained by digital analysis of the microfibre sample images are shown in Table 2 and

in Figure 2. A combination of factors determines the morphological characteristics of microfibres obtained by electrospinning, like the solution viscosity, the solvent physical and dielectric properties, the applied electrostatic force, and the viscoelastic response of the forming microfibres. The mean diameter of microfibres Mf-0 ($d = 3.61$ m) is in good agreement with literature data, considering the PVP concentration, the solvent, and the electrospinning conditions used [38].

The TEOS addition to the polymeric solution had an influence on the microfibres morphology due to the variation of the physical and dielectric properties of the obtained mixtures. The SEM images in Figure 1 show that irregular microfibres were observed only at the highest silicate concentrations as for samples Mf-18 and Mf-24.

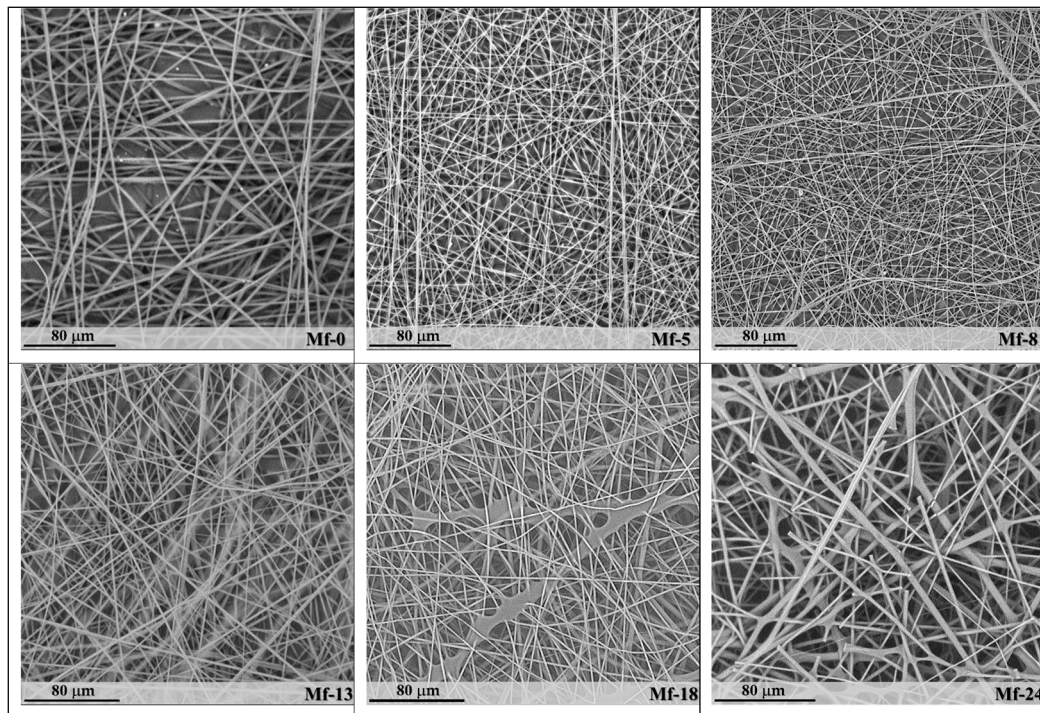


Figure 1. SEM images of microfibres coatings.

Table 2. Dimensional and compositional characteristics of the electrospun microfibres. Si wt.% (EDX) is the average value measured on the same regions of the SEM images of Figure 1.

Sample	Mean Diam. (m)	St. Dev. (m)	Initial Si wt.% (Dry Base)	Microfibres Si wt.% (EDX)	Error % (EDX)
Mf-0	3.61	0.86	0	0	0
Mf-5	1.25	0.23	4.3	4.0	3.3
Mf-8	1.54	0.37	6.7	5.8	3.2
Mf-13	2.13	0.52	11.8	12.6	1.6
Mf-18	3.14	0.56	16.8	26.1	1.3
Mf-24	5.52	1.72	23.4	28.0	1.2

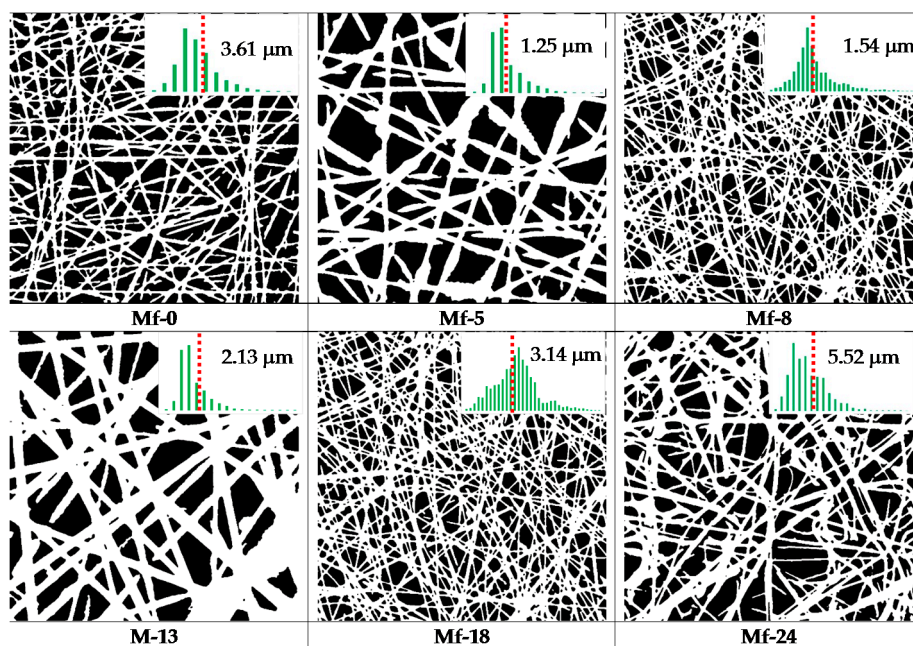


Figure 2. Determination of microfibre diameters by image digital analysis.

At low silicate concentrations, the hybrid microfibres from sample Mf-5 to Mf-13 resulted morphologically similar to the pure PVP microfibres, although they presented smaller average diameters with narrower size distribution than sample Mf-0 (Table 2). Increasing the TEOS concentration to 18 wt.% and 24 wt.%, the average diameter increased approaching the size of the pure PVP microfibres, however irregular formations were observed (Mf-18 and Mf-24 in Figure 1). A comparison between the silicon wt.% added in the precursor mixture before electrospinning and the Si wt.% measured on microfibres by EDX of Figure 1 is reported in Table 2. With TEOS being the only source of Si in the hybrid microfibres, the comparison between the two values is a further element for the evaluation of the mixtures electrospinnability. To be comparable, the initial Si concentration reported in Table 2 is calculated considering the dry weight, i.e., excluding the solvent.

In samples Mf-5 and Mf-8, the Si wt.% (EDX) in hybrid microfibres was slightly lower than the added amount, in sample Mf-13 it was slightly higher whereas in samples Mf-18 and Mf-24, at higher percentages of TEOS, the silicon concentration was clearly higher than in precursor mixtures. Comparing results in Table 2 and the SEM observations, it can be concluded that at silicate concentrations up to 13 wt.% the modification of the precursor solution characteristics, such as surface tension, viscosity, dielectric properties, had no negative effects on the formation of hybrid microfibres. According to several authors [4,38,44], the decrease of the average diameter of hybrid PVP microfibres observed in samples Mf-5 to Mf-13 has to be mainly attributed to an increase in the dielectric constant of solutions that contributed to the stretching of microfibres during ejection under the influence of electrostatic forces. The anomalous Si concentrations measured by EDX in samples Mf-18 and Mf-24, instead, are an indication that, when the TEOS content is increased beyond a certain quantity, difficulties in obtaining a good homogenization in the precursor mixtures emerged. The irregular formations shown in SEM images of samples Mf-18 and Mf-24 (Figure 1) are, indeed, areas where the EDX microprobe measured the highest Si concentrations.

3.2. Microfibres Thermal Characterization

Polyvinylpyrrolidone is obtained by the polymerization of a cyclic amide monomer (N-Vinylpyrrolidone) and has a high polarizability due to the carbonyl group in the amide ring (Figure 3). This characteristic determines the high-water affinity of PVP and it is the main reason

for selecting this material for the production of microfibres for adsorption systems driven by low temperature heat sources.

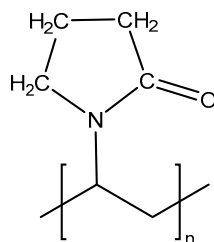


Figure 3. The polyvinylpyrrolidone polymeric unit.

In Figure 4, the thermogravimetric analyses of PVP microfibres in comparison with all other samples are shown. In the TGA-DSC plots reported, three main temperatures ranges have been identified as regions of principal thermal events: (I) for the temperature range $T = 25\text{--}150\text{ }^{\circ}\text{C}$, (II) for the range $T = 150\text{--}400\text{ }^{\circ}\text{C}$, and (III) for the range $T = 400\text{--}700\text{ }^{\circ}\text{C}$.

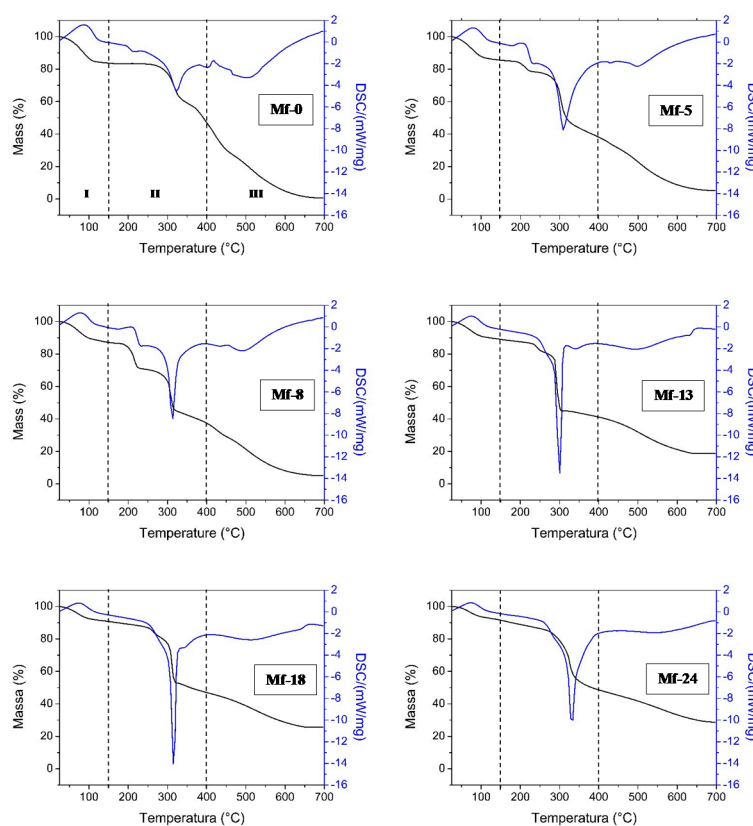


Figure 4. TGA-DSC plots of pure and hybrid polyvinylpyrrolidone (PVP) microfibre coatings.

In the low-temperature range (I), the sample Mf-0 plot (Figure 4) shows an endothermic peak associated to a mass loss that is due to the water desorption from the PVP microfibres. The same event is evident in all the samples (Figure 4) although as the Si concentration increases there is a shift of the endothermic peak towards lower temperatures (Table 3). Table 3 shows the weight loss at $T = 150\text{ }^{\circ}\text{C}$ for all the microfibres produced because a temperature $T \leq 150\text{ }^{\circ}\text{C}$ is used to regenerate the porous material, for example silica gel or SAPO-34, in low-temperature adsorption pumps [18,45] and $T = 150\text{ }^{\circ}\text{C}$ was considered, in this work, the reference temperature to evaluate the hybrid microfibres. Comparing the thermal behavior of a commercial silica gel (70-230 mesh, high purity grade, Sigma-Aldrich) to sample

Mf-0, the water adsorbed at 150 °C by PVP microfibres is even higher (Figure 5), which makes this material an interesting candidate for solid sorption at low temperature. In general, by increasing the Si concentration in the hybrid microfibres from sample Mf-5 to Mf-24, the water desorbed at $T = 150\text{ °C}$ decreased, as shown in Table 3.

Table 3. Thermogravimetric data from TGA-DSC plots in Figure 4.

Sample	Endothermic peak Temp. (°C)	Weight loss at $T = 150\text{ °C}$ (%)	Weight loss at $T = 400\text{ °C}$ (%)	Final Mass at $T = 700\text{ °C}$ (%)
Mf-0	87.0	16.4	50.2	0.6
Mf-5	80.9	14.6	61.6	5.2
Mf-8	80.7	13.0	62.3	5.4
Mf-13	74.7	11.0	60.4	18.1
Mf-18	74.4	9.4	53.8	25.6
Mf-24	73.8	8.6	52.3	28.7

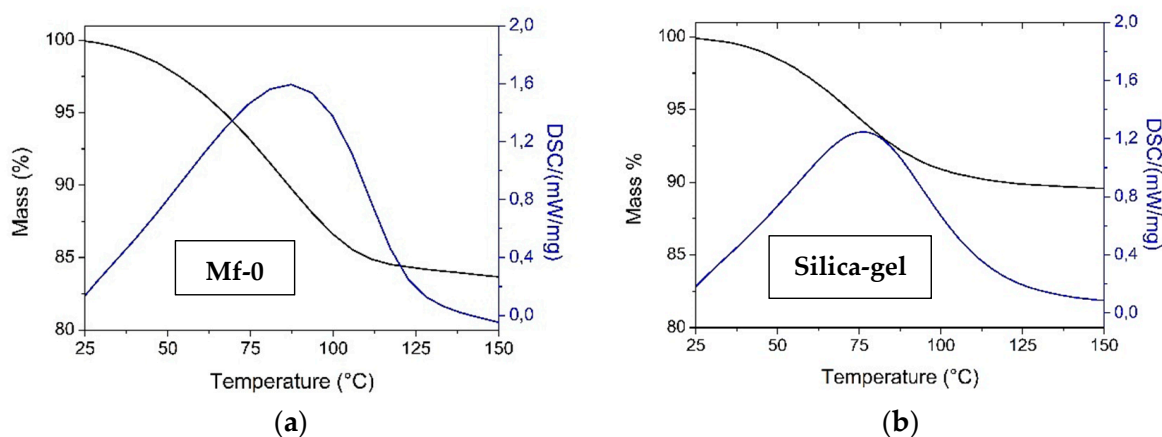


Figure 5. TGA-DSC comparison between pure PVP microfibres (a) and silica-gel (b) ($T = 25\text{--}150\text{ °C}$).

The TEOS addition, indeed, causes the bonding of siloxane species to the PVP carbonyl groups reducing the availability of polar bonds for water adsorption. A scheme of the TEOS interaction with the PVP polymeric chain for a low and high silicate concentration is shown in Figure 6. The lowest values of mass loss at $T = 150\text{ °C}$ (Table 3) were observed for microfibre samples with the highest Si concentrations (Table 2) due to the progressive addition of siloxanes (Figure 6).

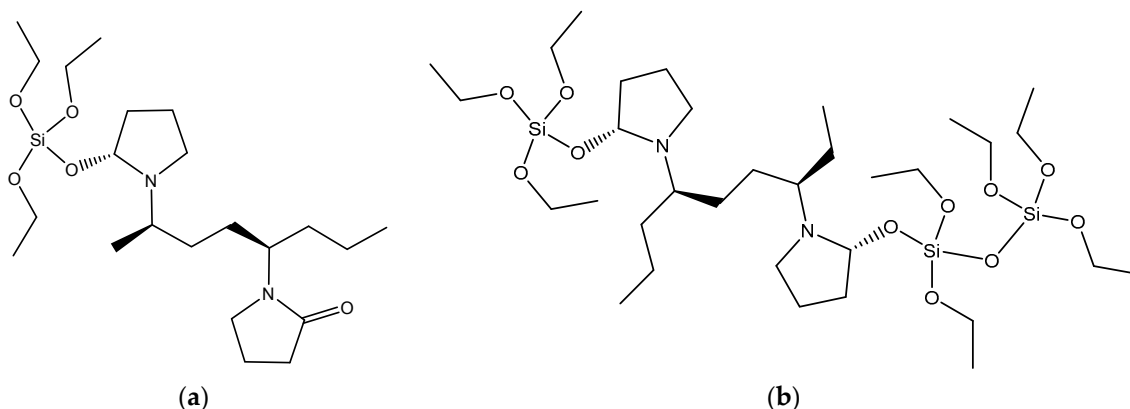


Figure 6. Schemes of the tetraethyl orthosilicate (TEOS) addition to PVP at low (a) and high (b) concentration.

In zone (II), two events are evident in all the plots of Figure 4. For pure PVP microfibrils, sample Mf-0, a first exothermic peak at $T > 200$ °C is followed by a more pronounced oxidation peak at $T = 323$ °C correlated to an evident mass decrease (~40%). The behavior of sample Mf-0 is in good agreement with literature data claiming a thermal degradation of the PVP pellets in air at $T \sim 400$ °C [36] although a slightly lower degradation temperature was observed for PVP microfibrils due to the greater surface area of microfibrils compared to pellets. In zone (II), for samples Mf-5 and Mf-8, the first peak associated to a mass loss at $T > 200$ °C is endothermic (Figure 4), followed by a more intense exothermic peak at $T \sim 300$ °C. The endothermic mass loss is an indication of the desorption of residual solvent trapped among the polymeric branches due to the availability of carbonyl groups given the low concentration of TEOS (Scheme a in Figure 6).

The exothermic peak at $T = 300$ °C instead, is related to the oxidation of PVP chains and the bond of siloxane species. Table 3 shows the mass loss of all microfibril samples at $T = 400$ °C. From sample Mf-0 to Mf-8, the increasing weight loss at $T = 400$ °C is related to the concurrent thermal degradation of the organic and inorganic components of the hybrid structure [46]. In the remaining samples Mf-13, Mf-18, and Mf-24 the first endothermic peak in zone (II) is not visible because increasing the Si content the exothermic peak at $T = 300$ °C becomes larger and more dominant (Figure 4). For these samples, the weight loss at $T = 400$ °C (Table 3) is always higher than that of sample Mf-0, however, it decreases increasing the TEOS used in the microfibrils. In sample Mf-18 and Mf-24, the lower weight loss at $T = 400$ °C is due to the high amount of siloxanes which, by binding to the surface of the microfibrils (Scheme b in Figure 6), delay the thermal degradation of the polymeric component.

Zone (III) in TGA-DSC plots shows the last thermal degradation of hybrid microfibrils characterized by an exothermic oxidation whose peak decreases from sample Mf-0 to Mf-24. For a comparison, in Table 3 are shown the residual weights at the final temperature of 700 °C. The final mass of pure PVP microfibrils is significantly lower than all other microfibril samples and from sample Mf-5 to Mf-24 the residual weight is similar to the Si wt.% measured by EDX (Table 2), confirming that the PVP component was almost completely decomposed at $T = 700$ °C. The difference between the final mass (18.1%) and the measured Si wt.% (12.6%) observed for Mf-13 microfibrils was due to an incomplete decomposition of the organic part of the sample.

The effect of the TEOS addition on the water adsorption capacity of PVP microfibrils is evidenced in Figure 7 where the weight loss at 150 °C is correlated to the Si concentrations shown in Table 2. Water molecules adsorb on PVP microfibrils by bonding to the carbonyl groups of the polymer chains. Their progressive saturation with the siloxane species of TEOS reduces the initial water affinity since the polarity of the hybrid, organic–inorganic system is reduced.

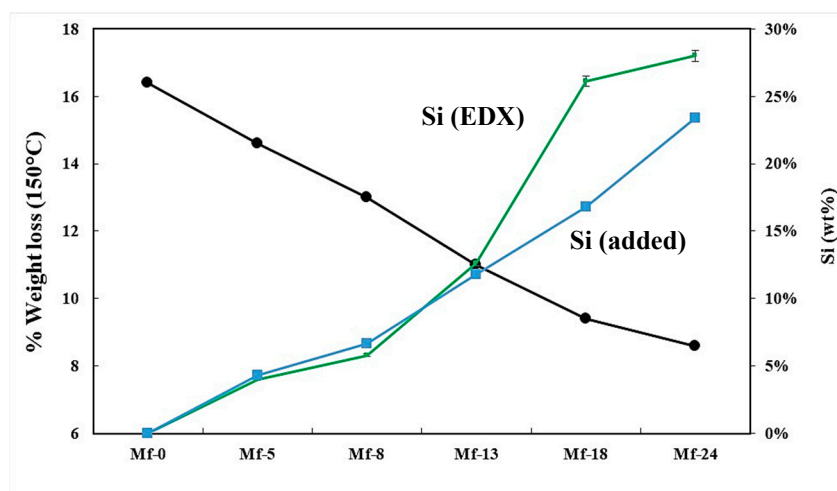


Figure 7. Correlation between weight loss ($T = 150$ °C) and Si concentrations for the electrospun microfibrils. Error bars of Si (EDX) measures are obtained from data in Table 2.

However, the reason for introducing such a modification in the original PVP microfibrils is related to the thermal stability that an adsorbent material must have under the cyclic adsorption and desorption of water vapor without showing any structural decomposition or loss of the initial water affinity. From this point of view, the unsaturated bonds of the PVP chains are sites of possible secondary (decomposition) reactions that could generate undesirable effects over time. To improve the thermal stability of PVP microfibrils, partial saturation of the carbonyl groups is advantageous although this costs in terms of adsorption capacity (Figure 7). From data in Figure 7, a good compromise is represented by samples Mf-5 and Mf-8 that have maintained a weight loss at $T = 150\text{ }^{\circ}\text{C}$ over 12%.

To evaluate the thermal degradation of hybrid microfibrils, a sample of Mf-5 microfibrils was exposed to a cycle of four TGA analyses in the following conditions: temperature range = 25–150 $^{\circ}\text{C}$, heating rate = 10 $^{\circ}\text{C}/\text{min}$ in airflow, holding time = 7 h at 25 $^{\circ}\text{C}$, and 45% RH at the end of each run. The results of the cyclic TGA test are shown in Figure 8. From the initial weight loss of 14.5% in Test 1, the second thermogravimetric curve showed a decrease to 13.5% (Test 2). Test 3 and the following Test 4, however, demonstrated a tendency of microfibrils Mf-5 to reach stable conditions for a final water desorption > 12.5 wt.%.

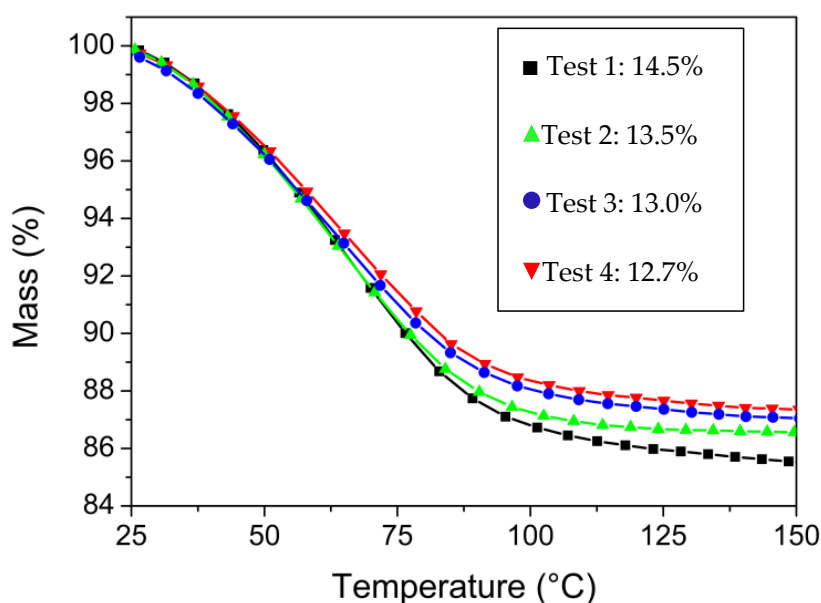


Figure 8. Cyclic TGA test for microfibrils Mf-5.

4. Conclusions

PVP is a polymer showing hydrophilic properties, so it could be an interesting adsorbing material for adsorption chillers driven by low temperature heat sources. An important advantage is the possibility of producing hybrid PVP microfibrils by electrospinning. This technique allows obtaining coatings made of microfibril layers, structured as non-woven mats, by an easy process. The implementation of microfibril coatings in adsorption technologies would bring clear advantages in terms of vapor permeability, large surface area, and mechanical strength, which is preserved by maintaining the hybrid, organic–inorganic structure of microfibrils. In order to increase the coating stability to the water adsorption/desorption cycles, PVP microfibrils were added with different amounts of TEOS. Silicate addition has shown to reduce the original water affinity of PVP, however, hybrid microfibrils with a TEOS concentration in the range of 5–13 wt.% demonstrated adsorption properties similar to commercial silica gel and a good short term thermal stability. Long term stability under many water adsorption/desorption cycles will soon be tested.

Author Contributions: Conceptualization, L.B. and P.F.; Investigation, A.M. and J.N.; Writing—Original Draft Preparation, A.M.; Writing—Review and Editing, M.K.

Funding: This research received no external funding.

Acknowledgments: The Authors are grateful to Luigi Calabrese and Edoardo Proverbio for their support and useful discussions.

Conflicts of Interest: The authors declare no conflict of interest.

References

1. Li, D.; Xia, Y.; Li, B.D.; Xia, Y. Electrospinning of nanofibers: Reinventing the wheel? *Adv. Mater.* **2004**, *16*, 1151–1170. [[CrossRef](#)]
2. Teo, W.E.; Ramakrishna, S. A review on electrospinning design and nanofibre assemblies. *Nanotechnology* **2006**, *17*, 89–106. [[CrossRef](#)] [[PubMed](#)]
3. Bhardwaj, N.; Kundu, S.C. Electrospinning: A fascinating fiber fabrication technique. *Biotechnol. Adv.* **2010**, *28*, 325–347. [[CrossRef](#)] [[PubMed](#)]
4. Angammana, C.J.; Jayaram, S.H. Fundamentals of electrospinning and processing technologies. *Part. Sci. Technol.* **2016**, *34*, 72–82. [[CrossRef](#)]
5. Leach, M.K.; Feng, Z.; Tuck, S.J.; Corey, J.M. Electrospinning fundamentals: Optimizing solution and apparatus parameters. *J. Vis. Exp.* **2011**, *47*, 1–5. [[CrossRef](#)] [[PubMed](#)]
6. Keun Kwon, I.; Kidoaki, S.; Matsuda, T. Electrospun nano- to microfiber fabrics made of biodegradable copolyesters: Structural characteristics, mechanical properties and cell adhesion potential. *Biomaterials* **2005**, *26*, 3929–3939. [[CrossRef](#)] [[PubMed](#)]
7. Ke, P.; Jiao, X.-N.; Ge, X.-H.; Xiao, W.-M.; Yu, B. From macro to micro: Structural biomimetic materials by electrospinning. *RSC Adv.* **2014**, *4*, 39704–39724. [[CrossRef](#)]
8. Kara, H.; Xiao, F.; Sarker, M.; Jin, T.Z.; Sousa, A.M.M.; Liu, C. Bio-based packaging. *J. Appl. Polym. Sci.* **2016**, *133*, 42475–42483.
9. Chakraborty, A.; Leong, K.C.; Thu, K.; Saha, B.B.; Ng, K.C.; Leong, C. Theoretical insight of adsorption cooling. *Appl. Phys. Lett.* **2011**, *98*, 2–4. [[CrossRef](#)]
10. Santori, G.; Luberti, M. Thermodynamics of thermally-driven adsorption compression. *Sustain. Mater. Technol.* **2016**, *10*, 1–9. [[CrossRef](#)]
11. Ge, T.S.; Wang, R.Z.; Xu, Z.Y.; Pan, Q.W.; Du, S.; Chen, X.M. Solar heating and cooling: Present and future development. *Renew. Energy* **2018**, *126*, 1126–1140. [[CrossRef](#)]
12. Meunier, F. Solid sorption heat powered cycles for cooling and heat pumping applications. *Appl. Therm. Eng.* **1998**, *18*, 715–729. [[CrossRef](#)]
13. Cacciola, G.; Restuccia, G. Reversible adsorption heat pump: A thermodynamic model. *Int. J. Refrig.* **1995**, *18*, 100–106. [[CrossRef](#)]
14. Flanigen, E.M. Molecular sieve zeolite technology—the first twenty-five years. *Pure Appl. Chem.* **1980**, *52*, 2191–2211. [[CrossRef](#)]
15. Castillo, J.M.; Silvestre-Albero, J.; Rodriguez-Reinoso, F.; Vlugt, T.J.H.; Calero, S. Water adsorption in hydrophilic zeolites: Experiment and simulation. *Phys. Chem. Chem. Phys.* **2013**, *15*, 17374–17382. [[CrossRef](#)]
16. Srivastava, N.C.; Eames, I.W. A review of adsorbents and adsorbates in solid–vapour adsorption heat pump systems. *Appl. Therm. Eng.* **1998**, *18*, 707–714. [[CrossRef](#)]
17. Bonaccorsi, L.; Calabrese, L.; Proverbio, E. Low temperature single-step synthesis of zeolite y coatings on aluminium substrates. *Microporous Mesoporous Mater.* **2011**, *144*, 40–45. [[CrossRef](#)]
18. Janchen, J.; Stach, H.; Ja, J. Shaping adsorption properties of nano-porous molecular sieves for solar thermal energy storage and heat pump applications. *Sol. Energy* **2013**, *104*, 16–18. [[CrossRef](#)]
19. Kohler, T.; Hinze, M.; Müller, K.; Schwieger, W. Temperature independent description of water adsorption on zeotypes showing a type V adsorption isotherm. *Energy* **2017**, *135*, 227–236. [[CrossRef](#)]
20. Ammann, J.M.; Michel, B.; Ruch, P.W. Characterization of transport limitations in SAPO-34 adsorbent coatings for adsorption heat pumps. *Int. J. Heat Mass Transf.* **2019**, *129*, 18–27. [[CrossRef](#)]
21. Henninger, S.K.; Jeremias, F.; Kummer, H.; Janiak, C. MOFs for use in adsorption heat pump processes. *Eur. J. Inorg. Chem.* **2012**, *2012*, 2625–2634. [[CrossRef](#)]

22. Yu, N.; Wang, R.Z.; Wang, L.W. Sorption thermal storage for solar energy. *Prog. Energy Combust. Sci.* **2013**, *39*, 489–514. [[CrossRef](#)]
23. Saha, B.B.; Uddin, K.; Pal, A.; Thu, K. Emerging sorption pairs for heat pump applications: An overview. *JMST Adv.* **2019**, *4*, 1–20. [[CrossRef](#)]
24. Goldsworthy, M.J. Measurements of water vapour sorption isotherms for RD silica gel, AQSOA-Z01, AQSOA-Z02, AQSOA-Z05 and CECA zeolite 3A. *Microporous Mesoporous Mater.* **2014**, *196*, 59–67. [[CrossRef](#)]
25. Demir, H.; Mobedi, M.; Ulku, S. A review on adsorption heat pump: Problems and solutions. *Renew. Sustain. Energy Rev.* **2008**, *12*, 2381–2403. [[CrossRef](#)]
26. Aristov, Y.I. Optimal adsorbent for adsorptive heat transformers: Dynamic considerations. *Int. J. Refrig.* **2009**, *32*, 675–686. [[CrossRef](#)]
27. Sapienza, A.; Gulli, G.; Calabrese, L.; Palomba, V.; Frazzica, A.; Brancato, V. An innovative adsorptive chiller prototype based on 3 hybrid coated/granular adsorbents. *Appl. Energy* **2016**, *179*, 929–938. [[CrossRef](#)]
28. Bendix, P.; Fuldner, G.; Möllers, M.; Kummer, H.; Schnabel, L.; Henninger, S. Optimization of power density and metal-to-adsorbent weight ratio in coated adsorbents for adsorptive heat transformation applications. *Appl. Therm. Eng.* **2017**, *124*, 83–90. [[CrossRef](#)]
29. Tatlier, M.; Erdem-Senatalar, A. Effects of metal mass on the performance of adsorption heat pumps utilizing zeolite 4A coatings synthesized on heat exchanger tubes. *Int. J. Refrig.* **2000**, *23*, 260–266. [[CrossRef](#)]
30. Schnabel, L.; Tatlier, M.; Schmidt, F.; Erdem-Senatalar, A. Adsorption kinetics of zeolite coatings directly crystallized on metal supports for heat pump applications (adsorption kinetics of zeolite coatings). *Appl. Therm. Eng.* **2010**, *30*, 1409–1416. [[CrossRef](#)]
31. Henninger, S.K.; Ernst, S.-J.J.; Gordeeva, L.; Bendix, P.; Fröhlich, D.; Grekova, A.D. New materials for adsorption heat transformation and storage. *Renew. Energy* **2017**, *110*, 59–68. [[CrossRef](#)]
32. Bonaccorsi, L.; Proverbio, E.; Freni, A.; Restuccia, G. In situ growth of zeolites on metal foamed supports for adsorption heat pumps. *J. Chem. Eng. Jpn.* **2007**, *40*, 1307–1312. [[CrossRef](#)]
33. Wittstadt, U.; Fuldner, G.; Laurenz, E.; Warlo, A.; Große, A.; Herrmann, R. A novel adsorption module with fiber heat exchangers: Performance analysis based on driving temperature differences. *Renew. Energy* **2016**, *110*, 154–161. [[CrossRef](#)]
34. Calabrese, L.; Bonaccorsi, L.; Freni, A.; Proverbio, E. Silicone composite foams for adsorption heat pump applications. *Sustain. Mater. Technol.* **2017**, *12*, 27–34. [[CrossRef](#)]
35. Malara, A.; Frontera, P.; Bonaccorsi, L.; Antonucci, P.L. Hybrid zeolite SAPO-34 fibres made by electrospinning. *Materials* **2018**, *11*, 2555. [[CrossRef](#)] [[PubMed](#)]
36. Peniche, C.; Zaldívar, D.; Pazos, M.; Páz, S.; Bulay, A.; Román, J.S. Study of the thermal degradation of poly(N-vinyl-2-pyrrolidone) by thermogravimetry–FTIR. *J. Appl. Polym. Sci.* **1993**, *50*, 485–493. [[CrossRef](#)]
37. Loria-Bastarrachea, M.I.; Herrera-Kao, W.; Cauich-Rodríguez, J.V.; Cervantes-Uc, J.M.; Vázquez-Torres, H.; Ávila-Ortega, A. A TG/FTIR study on the thermal degradation of poly(vinyl pyrrolidone). *J. Therm. Anal. Calorim.* **2011**, *104*, 737–742. [[CrossRef](#)]
38. Chuangchote, S.; Sagawa, T.; Yoshikawa, S. Electrospinning of poly(vinyl pyrrolidone): Effects of solvents on electrospinnability for the fabrication of poly(p-phenylene vinylene) and TiO₂ nanofibers. *J. Appl. Polym. Sci.* **2009**, *114*, 2777–2791. [[CrossRef](#)]
39. Huang, S.; Zhou, L.; Li, M.C.; Wu, Q.; Kojima, Y.; Zhou, D. Preparation and properties of electrospun poly(vinyl pyrrolidone)/cellulose nanocrystal/silver nanoparticle composite fibers. *Materials* **2016**, *9*, 523. [[CrossRef](#)]
40. Teo, W.-E.; Inai, R.; Ramakrishna, S. Technological advances in electrospinning of nanofibers. *Sci. Technol. Adv. Mater.* **2011**, *12*, 19. [[CrossRef](#)]
41. Jiang, F.; Dai, L.; Yao, Y. Polyamide 6-LiCl nanofibrous membrane as low-temperature regenerative desiccant with improved stability. *Nanotechnology* **2018**, *29*, 2–9. [[CrossRef](#)] [[PubMed](#)]
42. Huang, Z.M.; Zhang, Y.Z.; Kotaki, M.; Ramakrishna, S. A review on polymer nanofibers by electrospinning and their applications in nanocomposites. *Compos. Sci. Technol.* **2003**, *63*, 2223–2253. [[CrossRef](#)]
43. Hotaling, N.A.; Bharti, K.; Kriel, H.; Simon, C.G. Diameter]: A validated open source nanofiber diameter measurement tool. *Biomaterials* **2015**, *61*, 327–338. [[CrossRef](#)] [[PubMed](#)]
44. Shin, Y.M.M.; Hohman, M.M.M.; Brenner, M.P.P.; Rutledge, G.C.C. Experimental characterization of electrospinning: The electrically forced jet and instabilities. *Polymer* **2001**, *42*, 09955–09967. [[CrossRef](#)]

45. Chalaev, D.M.; Aristov, Y. Assessment of the operation of a low-temperature adsorption refrigerator. *Therm. Eng.* **2006**, *53*, 240–244. [[CrossRef](#)]
46. Da, Z.L.; Zhang, Q.Q.; Wu, D.M.; Yang, D.Y.; Qiu, F.X. Synthesis, characterization and thermal properties of inorganic-organic hybrid. *Express Polym. Lett.* **2007**, *1*, 698–703. [[CrossRef](#)]



© 2019 by the authors. Licensee MDPI, Basel, Switzerland. This article is an open access article distributed under the terms and conditions of the Creative Commons Attribution (CC BY) license (<http://creativecommons.org/licenses/by/4.0/>).